UNIVERSITYOF BIRMINGHAM

University of Birmingham Research at Birmingham

Integrated filter–amplifiers

Gao, Yang; Shang, Xiaobang; Li, Lei; Guo, Cheng; Wang, Yi

[Link to publication on Research at Birmingham portal](#)

Integrated Filter Amplifiers

[1]Yang Gao, *Member, IEEE*, [2]Xiaobang Shang, *Senior Member, IEEE*, [1]Lei Li, [3]Cheng Guo, *Member, IEEE*,

[4]Yi Wang, *Senior Member*, *IEEE*

[1]Zhengzhou University, Zhengzhou, China

[2]National Physical Laboratory (NPL), Teddington, UK.

[3]Xi'an Jiaotong University, Xi'an, China

[4]University of Birmingham, Birmingham, UK.

Emails : gaoyang678@outlook.com, xiaobang.shang@npl.co.uk, lilei@zzu.edu.cn, guocheng@xjtu.edu.cn, y.wang.1@bham.ac.uk

1. Introduction

Amplifiers and filters are essential components in microwave systems. An amplifier is used to increase the signal strength, and it is usually cascaded by filters for frequency selection or harmonic rejection [1]-[3]. Their functionalities require precise design of the individual parts as well as how they are connected. The common approach is to make individual components with a system impedance that is usually 50 Ω. A generic example of the filters and amplifier in a generalized receiver is shown in Figure 1(a).
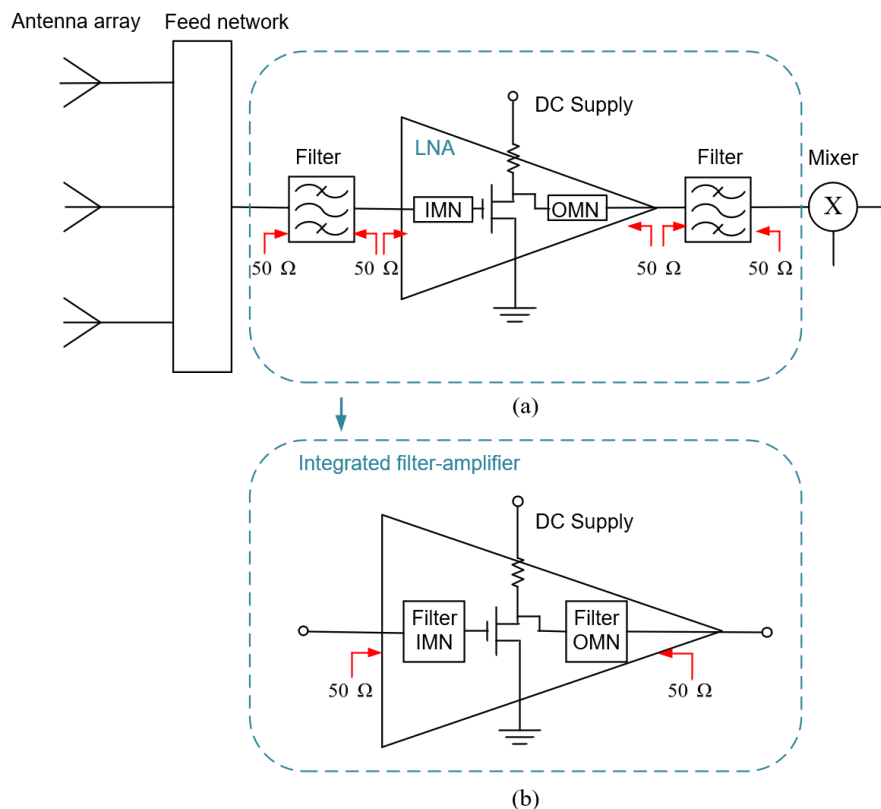
Figure 1. Illustration of (a) a typical receiver system and (b) an integrated filter-amplifier. The amplifier and filters can be integrated, eliminating the need for separate impedance matching circuits.

Rather than the conventional topology, where the amplifiers, matching networks and filters are separate, the amplifier and the filters can be integrated, allowing the input matching network (IMN) and the output matching network (OMN) of the transistor to be removed (see Figure 1(b)). In this approach, the filters are designed to replace the matching networks whose elements can be on-chip lumped circuits or planar structures. Thus, loss

1

reduction can be achieved through two aspects: first, the ohmic and dielectric loss of the microstrip matching circuitry can be minimized; secondly, the insertion loss and risk of multiple reflections associated with the port-to-port interconnection can be avoided. Apart from reduced loss, such integrated filter-amplifiers also have appealing advantages, such as significantly reduced size and improved performance in terms of matching and efficiency over the conventional approach based on individually cascaded components. These advantages are particularly attractive to millimeter-wave and terahertz (THz) applications, where the insertion loss of the matching network is usually a significant concern.

In this paper, we will review the recent advances of the integrated filter-amplifiers with featured techniques and examples being presented.

2. Extending passive filter design methods to active circuits

Passive filtersynthesis techniques have been well established [3]. These techniques normally deal with filters with real loads (usually 50 Ω), a valid assumption for typical microwave filters. However, in general, the loads presented by transistors are not real and present a complex frequency-dependent impedance, as shown in Figure 2(a). Filter-amplifier integration concerns the transformation of the transistor port impedances so that the amplifier response can be fully specified using Chebyshev, Butterworth, elliptical or other filtering functions (see Figure 2(b)). The challenge is to incorporate the complex impedances presented by the transistors into the design of passive filters where the real-valued source and load impedances are usually considered. The matching filters of the transistor also play an important role in the amplifier's characteristics such as efficiency, harmonic terminations, stability, and noise figure.
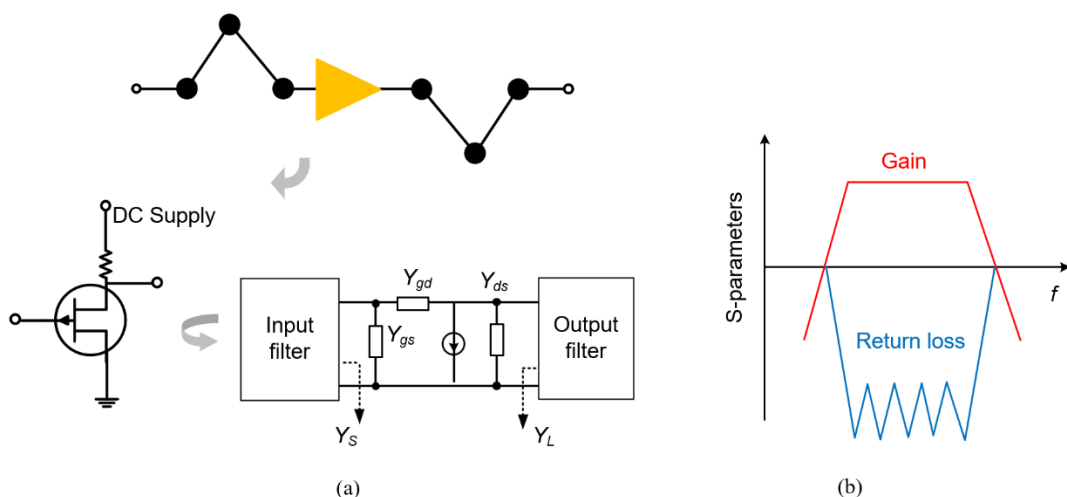
Figure 2. (a) Diagram showing filters matching the complex input and output impedances of a transistor. Y_S and Y_L are the optimum source and load admittances depending on types of the amplifiers; Y_{gd}, Y_{gs} and Y_{ds} are the admittances of the transistor small-signal model. (b) Illustrative filter-amplifier S-parameters response with a filtering function and gain.

Let us start the discussion with broadband filter-amplifiers, followed by the narrowband filter-amplifiers. For broadband amplifiers, matching filters are commonly realized using multi-stage LC elements-based ladder networks, enabling the use of the well-developed classic wideband filter synthesis. The matching filter design

techniques can be classified into numerical or analytical methods [4]. A numerical solution, namely the real frequency technique, was proposed by Carlin and Komiak [5] and further developed by Yarman and Carlin [6]. Fano, for the first time, came up with transcendental equations for broadband filter matching network with arbitrary impedance to achieve the desired return loss [7]. Dawson proposed the closed-form formulas and tabulated methods for broadband amplifier matching [8]. Other analytical techniques were also developed and utilized, such as clipping contour method [9], simplified real frequency technique [10], even–odd-mode analysis technique [11], and reactance compensation technique [12]. The distributed amplifier (DA) is also a common solution to broadband amplifications [13]. Different from the techniques discussed above, actively coupled resonators, active impedance/admittance inverters and negative-resistance were also applied to satisfy the filter transfer functions in DAs [13]-[15]. Compared with passive filter ladder-based amplifiers, the advantages of the DAs are flat gain, flat group delay, low noise figure, and low voltage standing-wave ratio (VSWR) over a wider bandwidth. The disadvantage of the active distributed filter is the need for multiple transistors which increase the circuit complexity and cost and result in relatively low efficiency.

Narrowband amplifiers deal with a relatively simpler situation because the complex frequency-dependent impedance can be treated as a constant value within the band of interest. By incorporating the arbitrary complex impedance of the transistor into the filter, the filtering matching can be readily maintained. There exist indirect and direct integration techniques for the filter-amplifiers. For the indirect approach, the imaginary component of the complex impedance is absorbed first and then transferred to the 50 Ω common terminal impedance. This is followed by the classic filter synthesis. The equivalent circuit analysis method can be employed in the conversion of arbitrary complex port impedance. In practice, coupled-lines [16] and quarter-wavelength impedance inverters [17] are often used in the conversion of the impedance's imaginary part, and the filter couplings are adjusted to match the real parts. The drawbacks of the indirect approaches lie in the additional circuit complexity and loss introduced by the transformation structure.
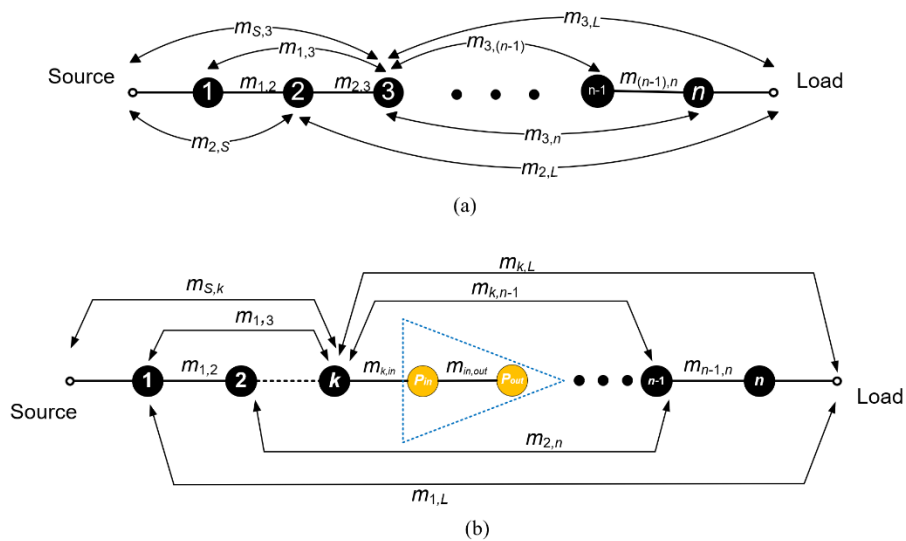

(a)

(b)

Figure 3. The general topology of (a) a passive filter and (b) an integrated filter-amplifier with coupling coefficients $m_{i,j}$ and a set of resonators labelled 1 to n showing couplings between the resonators. The active element (transistor) is represented by the non-resonating nodes P_{in} and P_{out}.

Different to the indirect approach, the direct filter-amplifier integration method treats passive elements and active elements as an entity and utilizes resonator-based filters to offer the matching for amplifiers. Figure 3 shows diagrams of a typical n-coupled resonator filter and an integrated filter-amplifier. In the resonator-based filter-amplifier topology, the complex impedance conversion can be achieved by choosing the appropriate coupling values [18]. For example, if the transistor has a complex input admittance $Y_{in} = a + jb$ (a and b are real constant), to achieve the desired Chebyshev (or other) filtering response, the coupling coefficients can be modified as [19]-[21],

$$m_{k,k} = -\frac{b}{a \cdot g_k g_{k+1}} \tag{1}$$

$$m_{k,in} = m_{in,k} = \sqrt{\frac{a^2 + b^2}{a \cdot g_k g_{k+1}}} \tag{2}$$

where g_k and g_{k+1} are the standard g values defined in the Chebyshev low-pass prototype [3]. $m_{k,k}$ is the self-coupling of the kth resonator which is adjacent to the transistor port; $m_{k,in}$ and $m_{in,k}$ are the couplings between the kth resonator and the transistor.

This resonator-based filter integration technique is ideally suitable for applications at millimeter-wave and terahertz frequencies in that the loss could be very low if the resonators are made from high-Q waveguide structures [22]-[24]. Resonator-based filter matching approaches can also be employed to provide the desired matching for other types of microwave circuits with complex port impedance. For example, we have demonstrated this on filter-amplifiers with different topologies [19]-[21], orthomode transducers [25], Schottky diode-based frequency triplers [26], [27] and subharmonic mixers [28].

Sidebar-1: Active coupling matrix synthesis for filter-amplifiers

The concept of the coupling matrix was first introduced by A. Atia and A. Williams in the 1970s and implemented using waveguide cavity filters [29]. Initially, an $N \times N$ matrix design approach was developed based on lumped circuit elements and ideal transformer coupling. This was later extended to the $N+2$ coupling matrix with port impedances were included [30]. Recently, $N+3$ and $N+4$ active coupling matrices based on direct-synthesis and optimization methods were developed [19]-[21] to deal with the design of filter-amplifiers. The typical $N+2$ passive coupling matrix and the recently-developed active coupling matrix elements are illustrated in Figure S1.

(a)

(b)

Figure S1. General coupling matrix of (a) a passive filter and (b) an integrated filter-amplifier. Note that the active coupling matrix includes the active transistor elements $m_{in,out}$ and $m_{out,in}$, which represent the couplings (or feedback) between the transistor's input and output. $m_{i,j}$ represents the inter-resonator coupling; $m_{S,j}=m_{j,S}$ and $m_{L,j}=m_{j,L}$ (j=1 to n) are the coupling from the source and load; $m_{j,in}=m_{in,j}$ and $m_{out,j}=m_{j,out}$ are the couplings from the resonators to the transistor's gate and drain.

Three topology examples and their corresponding S-parameters responses are given in Figure S2. Their coupling matrices can be directly synthesized for filter matching with a Chebyshev response, when resonators are coupled to the input or output of the transistor, as shown in Figure S2(a) and (b). When the transistor is placed between resonators, as shown in Figure S2(c), the coupling matrix can be obtained using the optimization method [21]. This is due to the existence of feedback from the transistor, making it more difficult to calculate the coupling coefficients using the direct synthesis technique. Apart from S-parameters, noise figures have also been derived using the coupling matrix technique [21]. It is worth noting that the active coupling matrix approach can also be applicable to other amplifier parameters such as stability factor,

gain and efficiency. The active coupling matrix represents a new and potentially generic design approach for filter-amplifiers and other types of active and non-linear circuits.
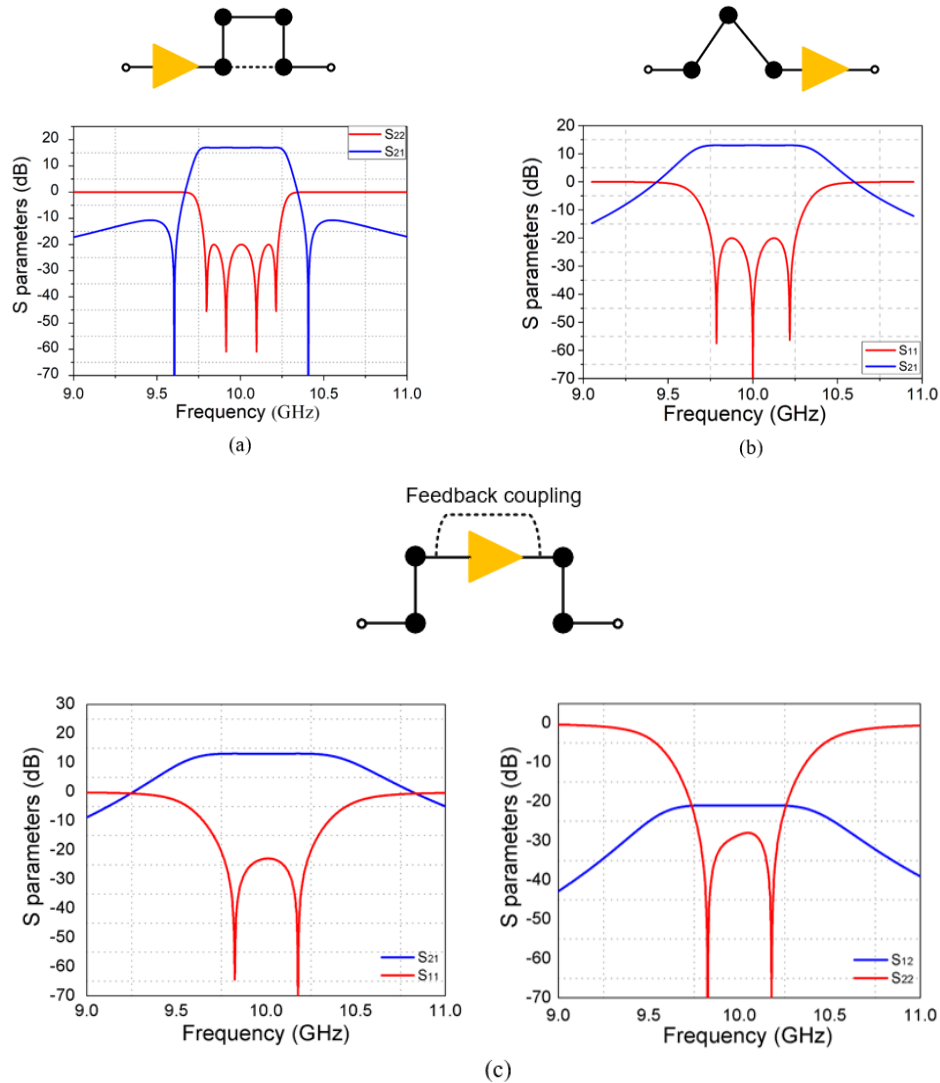
Figure. S2 Examples of filter-amplifier topologies and their corresponding S-parameters responses where resonators coupled (a) to the input of the transistor; (b) to the output of the transistor; (c) to both sides of the transistor.

3. Physical construction of integrated filter-amplifiers

Now let us move onto the practical amplifier design. Electrical and physical characteristics of the integrated filter-amplifiers are closely related to the transistors, the packaging process, choice of filter types and integration techniques. It should be noted that the design of the filter-amplifier is a two-stage approach, where the type of filter (e.g. microstrip, coaxial, waveguide, dielectric) can be considered at the second stage. The technique described here can be used in different types of filters. The choice of the filter types depends upon the device or system requirements such as insertion loss, achievable bandwidth, power handling capability, noise, power, temperature stability, size, and cost. Physical construction of the filter and how they are integrated with the on-chip transistor is an important practical consideration. A few different schemes of filter-amplifier integration using various physical structures will be reviewed later.

6

TABLE I
TYPICAL Q-FACTORS OF VARIOUS TYPES OF RESONATORS [31]

	Microstrip/ Stripline	Substrate Integrated Waveguide (SIW)	Dielectric Resonator	Rectangular Waveguide
Unloaded Q-factor	50-200	150-1000	200-3000	1000-12000

The losses of the integrated filters (including dielectric loss, ohmic loss, and radiation loss) are not only determined by the physical and electrical parameters of the materials but also by their physical construction. Table I summarizes the typical unloaded Q-factors of several popular microwave resonators. Advanced manufacturing technologies allow various physical construction being precisely fabricated. Apart from traditional CNC machining, emerging manufacturing technologies such as 3-D printing, SU-8, laser-cutting, and silicon DRIE have been utilized in making various passive microwave circuits [32]. Combining these advanced machining technologies with the new packaging and integration scheme is expected to greatly reduce the loss and improve the efficiency of the amplifier and advance the technologies into new applications at increasingly high frequencies.

3.1. Microstrip filter-amplifiers

Planar circuit filters are commonly used for matching transistors, for their low production cost and ease of fabrication [33]-[37]. Compared with nonplanar metallic structures, planar matching filters bring in relatively high losses. As frequencies go higher to the sub-millimeter or terahertz regime, the losses increase rapidly and impair the amplifier's performance. Therefore, planar filter-amplifiers are often found in relatively low frequency applications.

Figure 4 shows a schematic of a narrowband microstrip power amplifier with a filter integrated at the transistor output [33]. The equivalent circuit analysis technique is used. Through a microstrip tuning line, the imaginary part of transistor impedance can be absorbed. The normalized real input impedance was obtained using the coupling coefficients, expressed by

$$Z_{in} = \frac{M_{1,2}^2}{M_{S,1}^2 M_{2,L}^2} \tag{3}$$

To fulfil the required input impedance Z_{in}, the external coupling can be adjusted by controlling external quality factor Q_e, according to

$$M_{S,1} = \frac{1}{\sqrt{Q_e \cdot FBW}} \tag{4}$$

The embedded filtering circuit not only realized the impedance matching at the operating frequency but also eliminated the harmonics. Figure 5(a) shows the simulated and measured S-parameters results, showing a gain of around 16.4 dB over the passband. Two transmission zeros (TZs) are created at the passband edges to

enhance the selectivity. Figure 5(b) gives the simulated and measured P_{out}, gain and power-added efficiency (PAE) of the power amplifier at a fixed frequency of 2.45 GHz. The PAE is up to 69.8%, and the corresponding output power and gain are 40.1 dBm and 11.8 dB, respectively. With the integrated filter, the skirt selectivity is increased, and the total size of the integrated component is $0.65\lambda_g \times 0.48\lambda_g$, smaller than the cascaded power amplifier and filters.
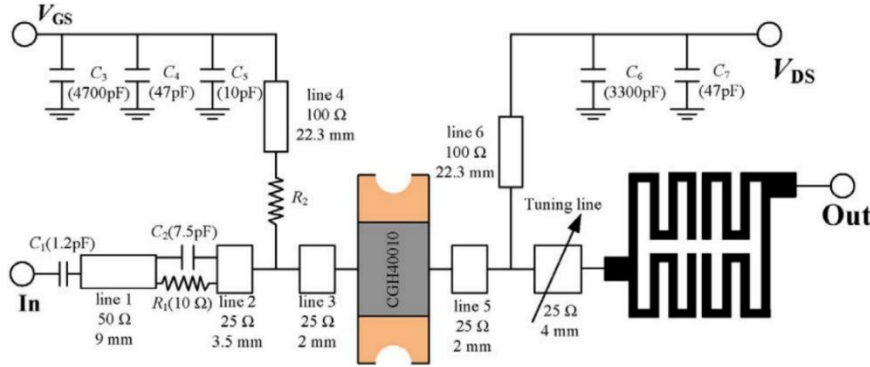
Figure 4. Schematic of the power amplifier integrated with a filter at its output [33].
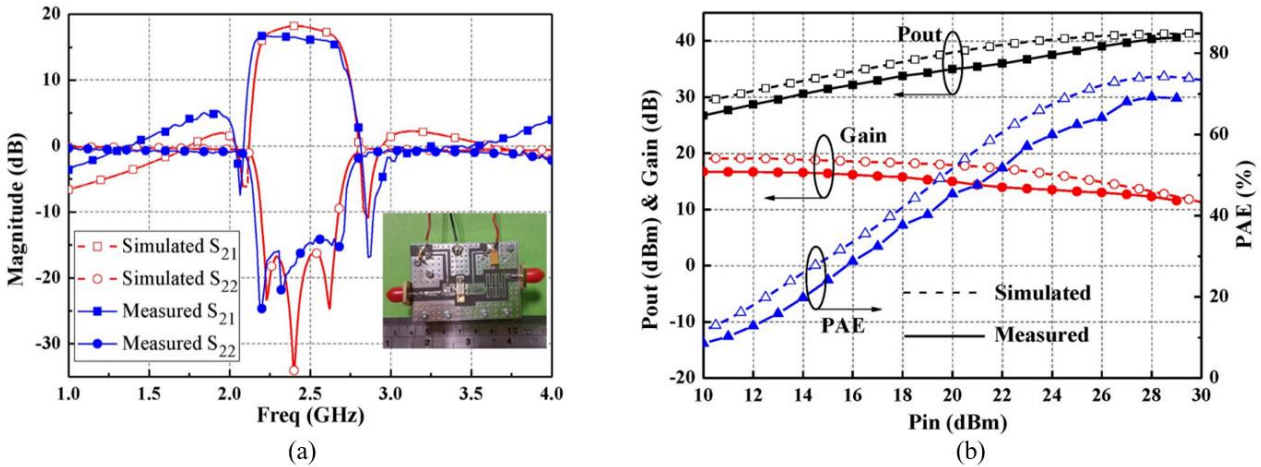
Figure 5. Performance of the filter-amplifier shown in Figure. 4. (a) Simulated and measured S-parameters. (b) Simulated and measured P_{out}, gain and power-added efficiency (PAE) [33].

3.2. Substrate integrated waveguide (SIW) filter-amplifiers

SIW becomes an attractive candidate transmission media as frequencies go higher due to its lower loss than microstrip circuits. SIW technology usually presents good performance for applications under 100 GHz. Also, the good manufacturability of SIW provides a unique and attractive solution for mass-production or cost-sensitive applications, even though the Q-factor (150-1000) of SIW resonators is generally lower than metallic waveguide resonators (1000-12000).

As a planar structure, SIW is easy to integrate with on-chip active devices. Specifically, broadband amplifiers can be more feasibly achieved using SIW matching structures because it supports propagation of TE modes

and avoids parasitic TM modes. De-embedded coupling slots and stepped impedance transitions are often used in controlling external coupling strength for impedance transformation. The inter-resonator couplings are commonly implemented by using irises.

Evanescent (EVA) mode cavity resonators based on SIW technology have been utilized for the design of the narrowband power amplifier's OMN in [24]. The circuit diagram and the physical construction are illustrated in Figure 6. The coupling coefficients are determined by the geometries of the coupling iris and the external couplings are realized using slot apertures. By tuning the bias line, the second harmonic is terminated in the high-efficiency region while the fundamental impedance almost remains the same. The small and large-signal responses of the filter-amplifier are given in Figure 7. Note that the co-design approach enhances the efficiency from 64% (cascaded) to around 72% (co-design) at a power saturation of 40 dBm.

(a)   (b)
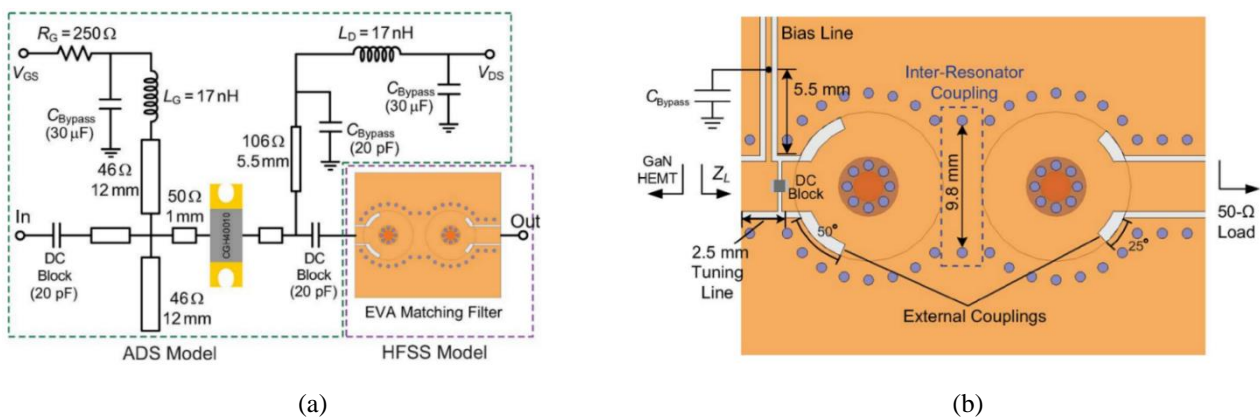
Figure 6. (a) Circuit schematic of the co-designed filter-amplifier. (b) Construction of the two-pole SIW filter [24].

(c)
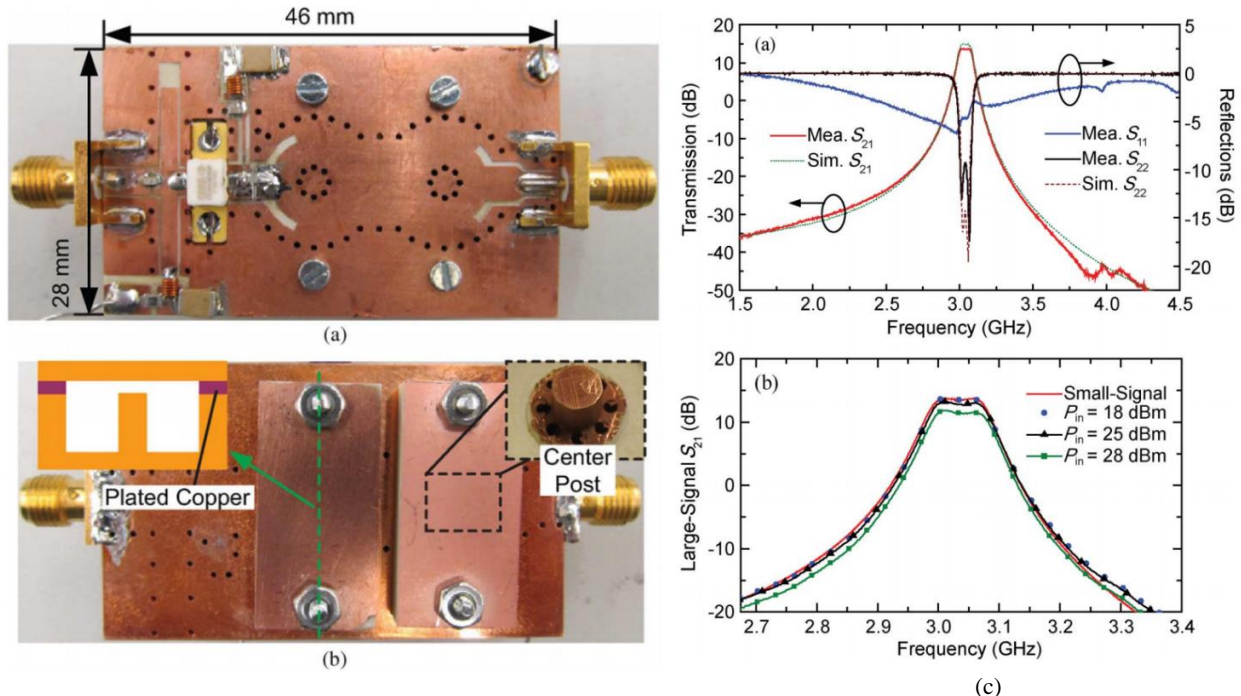
Figure 7. Photos of the fabricated SIW filtering power amplifier. (a) Front side; (b) backside; (c) measured and simulated small and large-signal results of the device [24].

A more general filter-amplifier topology is given in [21], where an all resonator structure is applied to replace both the IMN and OMN of the transistor, as illustrated in Figure 8. The amplifier geometries can be extracted accurately using the coupling matrix which resembles the classic passive filter design method. The size of the coupling iris (w_i in Figure 8) can be determined from the coupling coefficients. As shown in Figure 9, the two-pole Chebyshev responses are displayed in both S_{11} and S_{22} responses; S_{21} shows about 9-dB gain over the passband; and the measured noise figure is around 2.5 dB in the passband. Different from the previous examples where the input and output matching filters are modelled individually, the feedback coupling between output and input in the transistor is considered in [21]. This provides an integrated design method, for which the physical geometrics can be extracted more accurately, yielding much reduced electromagnetic simulation time.

(a)

(b)

(c)

Figure 8. (a) Layout of the SIW filter-amplifier. (b) Schematic of the filter matching at the input and output of the transistor. (c) Photo of the fabricated SIW filter-amplifier [21].

Figure 9. Simulation and measurement results of the filter-amplifier shown in Figure 8. (a) S_{11} and S_{21}; (b) S_{22} and S_{12}; (c) noise figure; (d) 1 dB compression point (P1-dB) measurement [21].

3.3. Waveguide filter-amplifiers

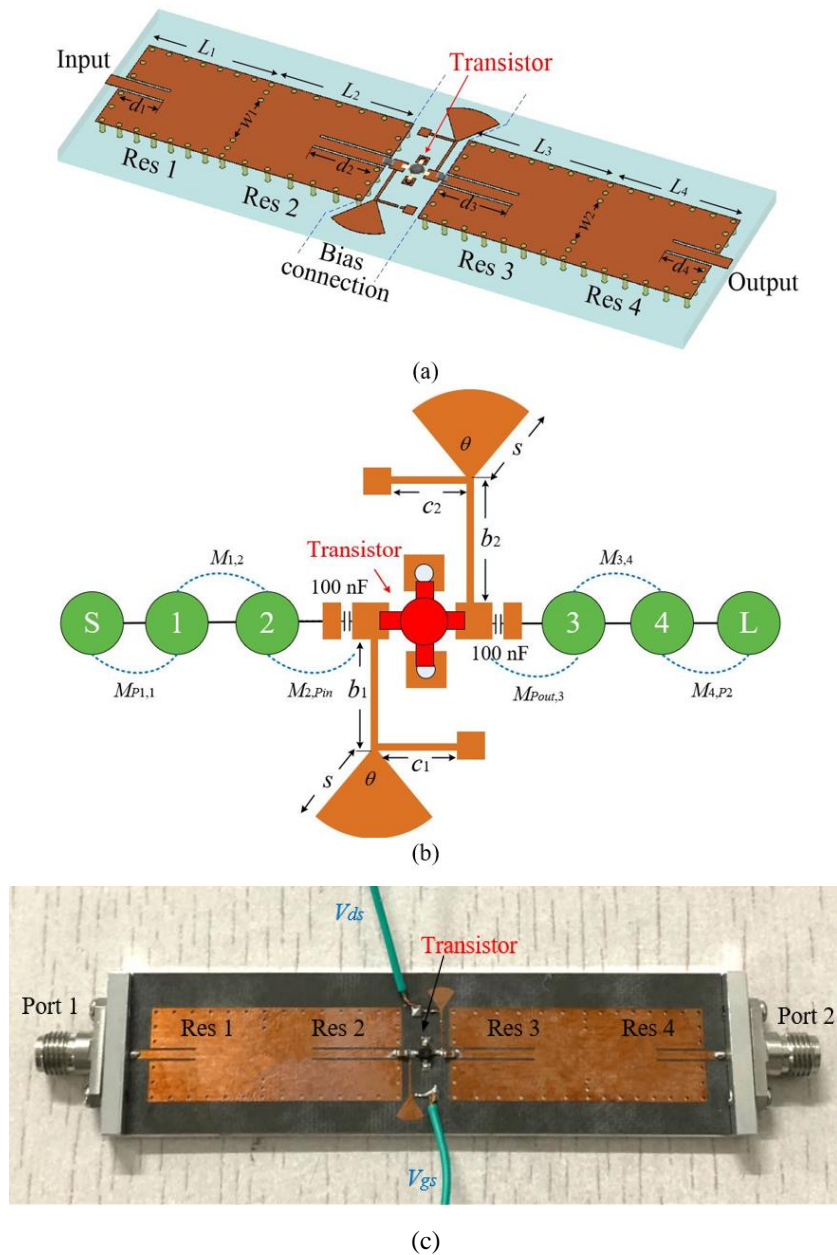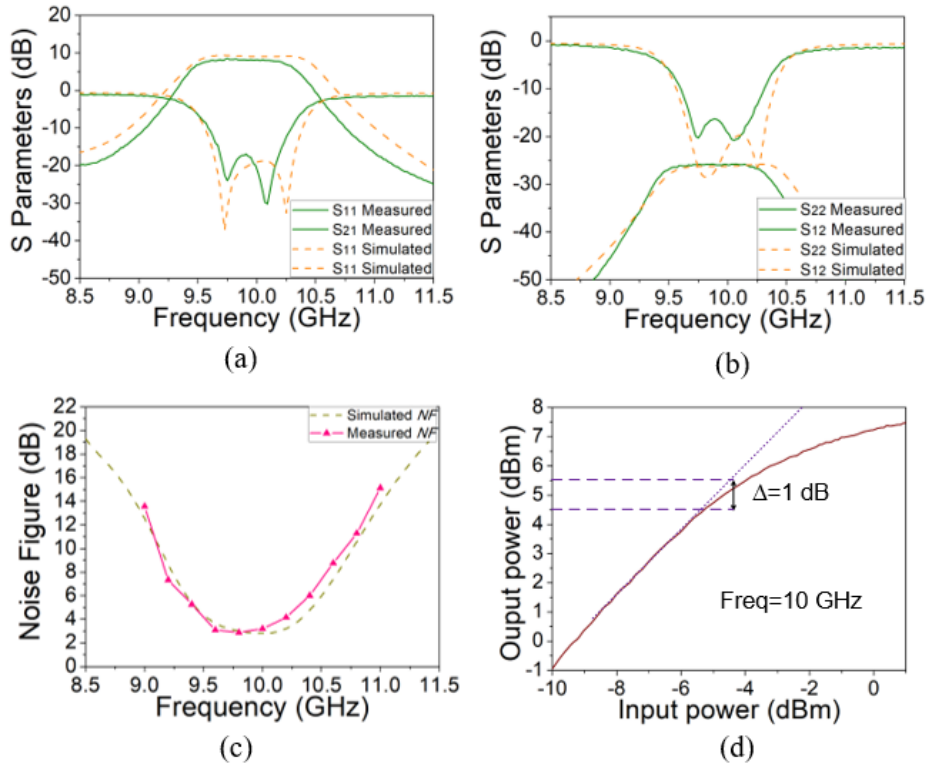If the even higher frequency or power capacity must be fulfilled in the amplifier applications, the use of high-performance non-planar components become imperative. The metallic waveguide featuring high-Q is an attractive structure at higher frequencies, especially for millimeter-wave and THz applications. Three-dimensional metallic filters in the form of rectangular, cylindrical or spherical shapes are usually selected for loss-sensitive, high performance, and high-power capacity applications [19], [22], [38]. The main disadvantage is that the structure is bulky in size and the manufacturing could be costly. One challenge of using three-dimensional metallic waveguides is the transition between on-chip transistor and waveguide. Transition structures with high coupling efficiency are not easy to realize. E-plane probes, dipoles, and finlines are the common choices of the transitions. Other contactless or air-filled transitions, such as step ridges, can avoid dielectric loss, with the penalty of increased complexity and cost. For waveguide filter-amplifier integration, active inverters or resonators methods discussed above no longer apply, because it is difficult to model active elements within three-dimensional construction.

Figure 10 illustrates a tunable filtering power amplifier where the resonators are tuned using screws [23]. The center frequency can be tuned from 2.95 GHz to 3.35 GHz, as shown in Figure 11. The power efficiency reaches its highest point of 67% and the corresponding gain compression is about 2 dB at the maximum output power of 40 dBm.
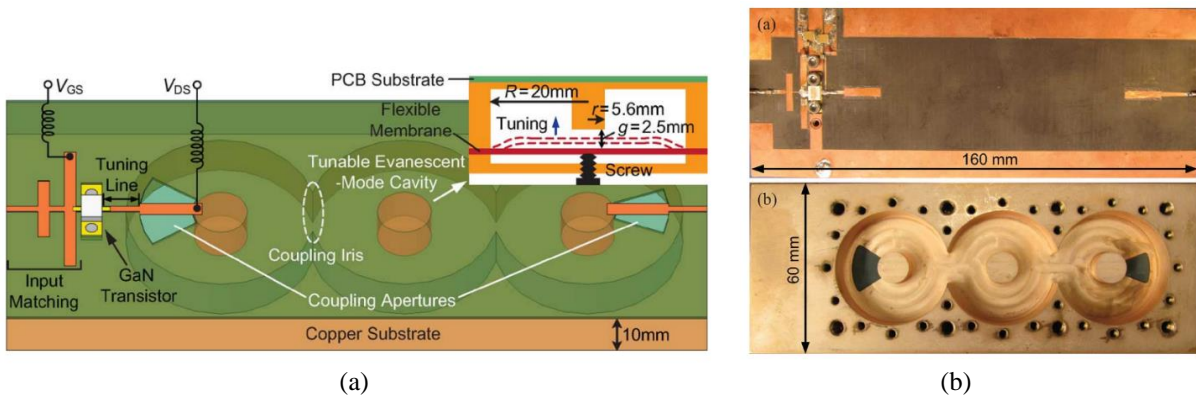
Figure 10. (a) Physical construction of the power amplifier with a tunable three-pole evanescent-mode filter. (b) Photos of the fabricated filter integrated power amplifier [23].

Figure 11. Performance of the filter-amplifier in Figure 10. (a) Measured and simulated S-parameters; (b) Measured output power and gain versus input power at 3.1 GHz [23].

Figure 12 shows a waveguide filter-amplifier with E-plane probes used for coupling the waveguide and the transistor [20]. The inter-resonator couplings are achieved by the waveguide iris, while the external couplings are determined by the probe structure. The photo of the waveguide amplifier is shown in Figure 13. The measured results in Figure 14 show the Chebyshev filtering response of S_{11} and S_{22}. The S_{21} curve indicates a gain of around 11.1 dB over the passband. The brief design procedure of such waveguide filter-amplifier is described in Sidebar-2.
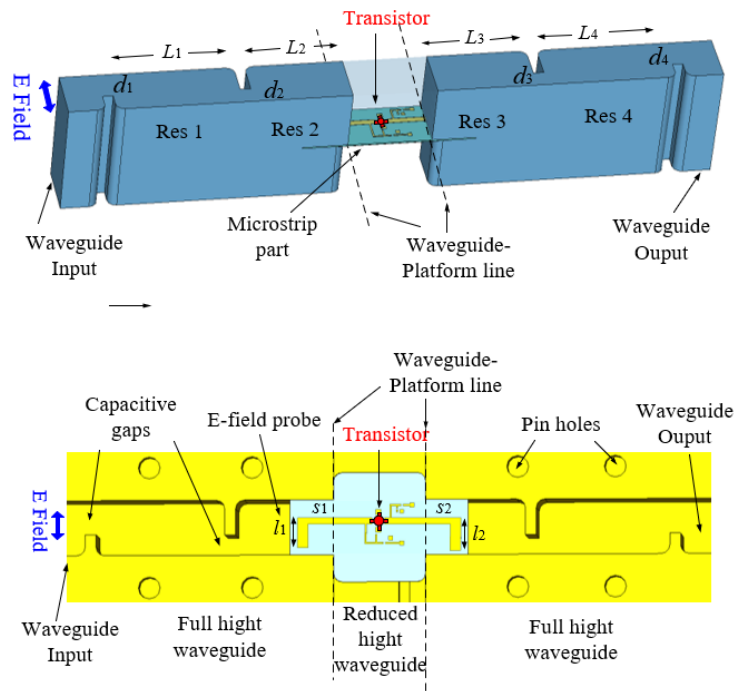
Figure 12. Diagrams of the waveguide filter-amplifier [20].
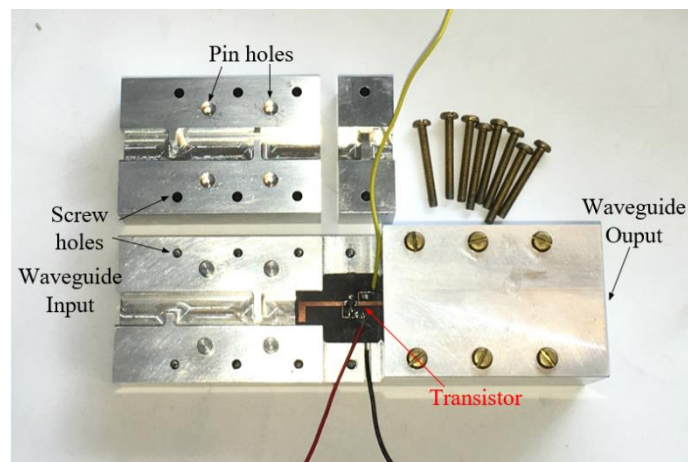
Figure 13. Photograph of the fabricated waveguide filter-amplifier [20].
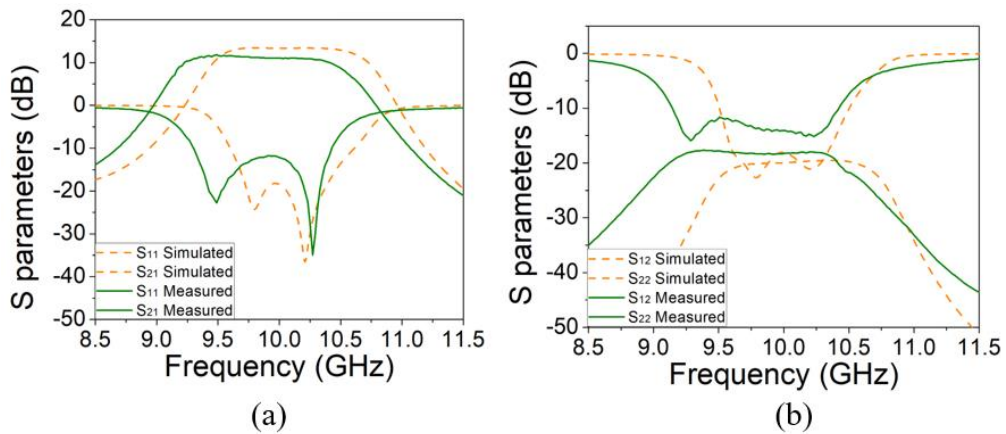
Figure 14. Simulation (dashed lines) and measurement (solid lines) results of the filter-amplifier in Figures 12 and 13. (a) S_{11} and S_{21}; (b) S_{22} and S_{12} [20].

13

3.4. Dielectric resonators filter-amplifiers

Dielectric resonators (DRs) feature a high-Q factor and lower cost than waveguide cavities [39], [40]. As illustrated in Figure 15, a dielectric resonator filter was employed to realize output impedance matching of the gallium nitride (GaN) transistor power amplifier [40]. The analytical method was used for the DR-based filter-amplifier design. To realize the filtering response, a transmission line TL11 is used to eliminate the imaginary part of the load impedance. The DR filter converts the real impedance to 50 Ω through tuning the external couplings, as given by [40]

$$M'_{S,1} = \frac{M_{S,1}}{\sqrt{R_{in}}} \tag{5}$$

The filter's selectivity was enhanced by the two transmission zeros (TZs) near the passband. This integrated DR filter-amplifier achieves a small-signal gain of 18.3 dB with 3 dB bandwidth of 2.3%. The measured P_{out}, PAE, and drain efficiency at 1.88 GHz are given in Figure 16. This filter-amplifier exhibits its superiority of high PAE over the microstrip filter-amplifier in [33] and the hybrid microstrip-cavity filter-amplifier in [38] with the same fractional bandwidth.
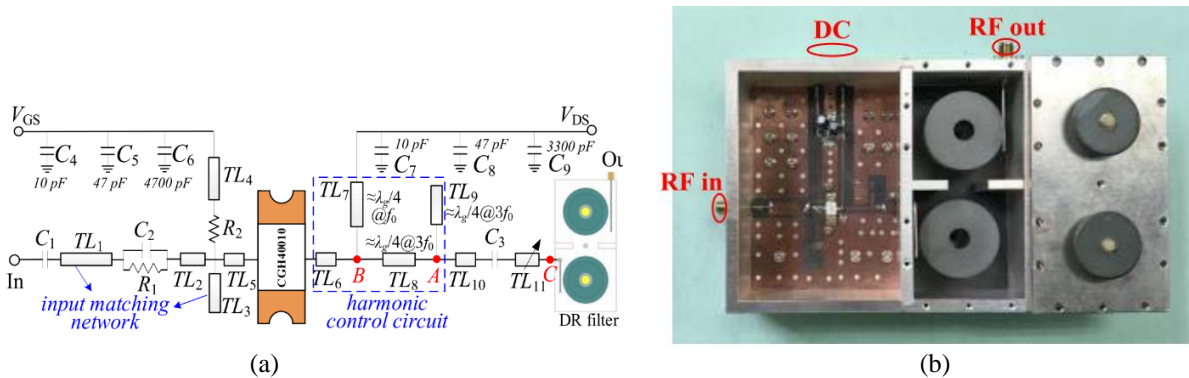
Figure 15. (a) Configuration of the DR filtering power amplifier; (b) Photograph of the fabricated device [40].

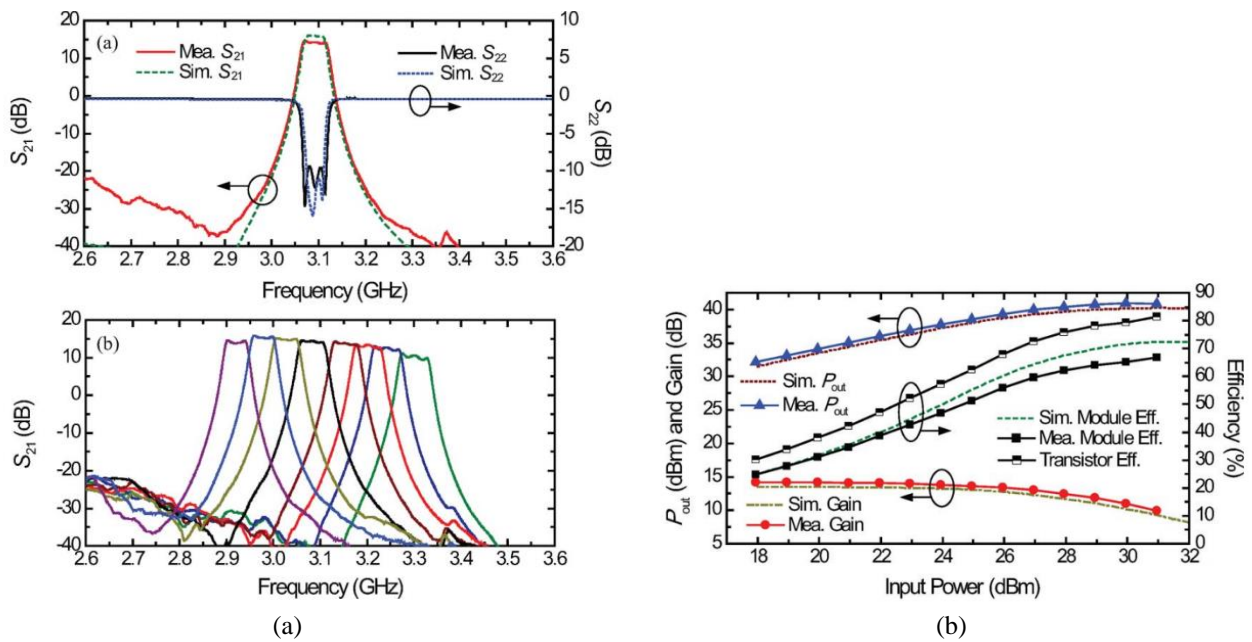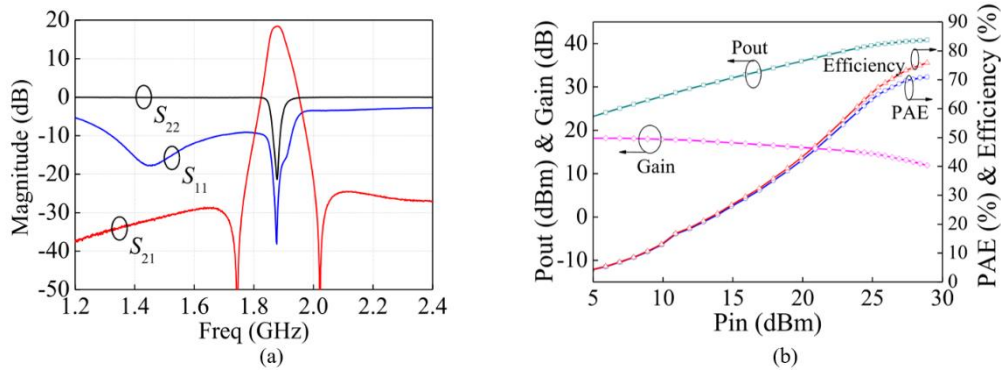Figure 16. Performance of the filter-amplifier in Figure 15. (a) Measured and simulated S-parameters; (b) Measured P_{out}, gain, efficiency, and power-added efficiency (PAE) versus input power [40].

4. Broadband filter-amplifiers

Broadband filter synthesis methods used to match the frequency-dependent impedance of amplifiers have already been reviewed briefly above. In this section, a broadband filter-amplifier is presented as an example, and several recently published broadband filtering amplifiers are summarised in Table II. In general, the required wideband matching networks are commonly realized using passive LC-ladder networks, which are usually based on microstrip structures.

TABLE II
SUMMARY OF RECENTLY PUBLISHED BROADBAND FILTERING POWER AMPLIFIERS

Mode	BW (GHz, %)	P_{out} (dBm)	Eff. (%)	Gain (dB)	Filter Matching Technique	Ref.
Class-J	2-3, 40	40-41.8	58-72	11.5-12.5	Equivalent circuit nonlinear model approximation	[4]
n/a	1.9-4.3, 78	39.5- 41.8	57-72	9-11	Resonant parallel LC circuits	[9]
Class-F	1.45-2.45, 51	35.7-35.9	70-81	10-12.6	Simplified real frequency technique	[10]
n/a	0.8-3.2, 120	39.7- 42.9	57-74	10.7-13.5	Even–odd-mode analysis technique	[11]
Class-E	0.136-0.174, -	39.03	74	11.5-12.2	Reactance compensation technique	[12]
Class-J	1.4-2.6, 60	39.5- 40.4	57-72	11-12	Norton transformer	[41]
n/a	1.2-2.3, 63	40.6-42.6	64.3-77.5	12.4-14.5	D/CRLH bandpass filter	[42]
n/a	2-4, 70.7	35.1-38.9	40-55	9.5-11	Minimum inductor bandpass filter	[43]
n/a	1.9-2.3, -	39-40.4	69-78.2	13.4-15.1	Coupled line based tuning network	[44]
Class-F	1.35-2.5, 60	40.96-42.6	68-82	15.2-17	Modified elliptic low-pass filter	[45]
Class-E	1.4-2.7, -	39-41.2	64.5-73.5	9-10.9	Shunt capacitance and shunt filter	[46]
Class-E	0.9-2.2, 84	40-43	63-89	10-13	Synthesized low-pass matching network	[47]
n/a	1.7-2.6, 35	28-42	65-78	9.1-10.1	Step-impedance quasi-Chebyshev lowpass filter synthesis	[48]
Class-F	0.3-1, 107.7	37-40.3	62-81	12-15.3	Quasi-elliptic low-pass filtering network	[49]
n/a	1.15–2.45, 77.4	39.7-41.7	38.4- 52.2	6.5	Optimum balanced broadband load network	[50]

15

Figure 17 shows an example of broadband filtering power amplifier [42], employing a right-/left-handed (CRLH) cell and a dual CRLH (D-CRLH) cell that offer filter matching to the amplifier. Matching filters formed by the D-CRLH absorb the bias circuits and allow for reduced circuit footprint. Note that filter matching at both the fundamental and harmonic frequencies is required over the bandwidth. An optimum impedance of 19.7+5.5j Ω at the center frequency of 2 GHz was chosen. The real-to-real and real-to-complex transformations were carried out. The measured S-parameters of the filter-amplifier are given in Figure 18(a), where return loss is around 5 dB and a transmission zero is created at 3 GHz. The measured drain efficiency (DE) and output power versus frequency at an input power of 28 dBm are shown in Figure 18(b). Compared with conventional LC-ladder based lowpass matching filters, the D-CRLH bandpass filter matching network demonstrates its broadband harmonic impedance transformation characteristics.

(a)

(b)

Figure 17. (a) Schematic of the broadband power amplifier. (b) Prototype of the proposed broadband power amplifier using D-CRLH BPF matching method [42].
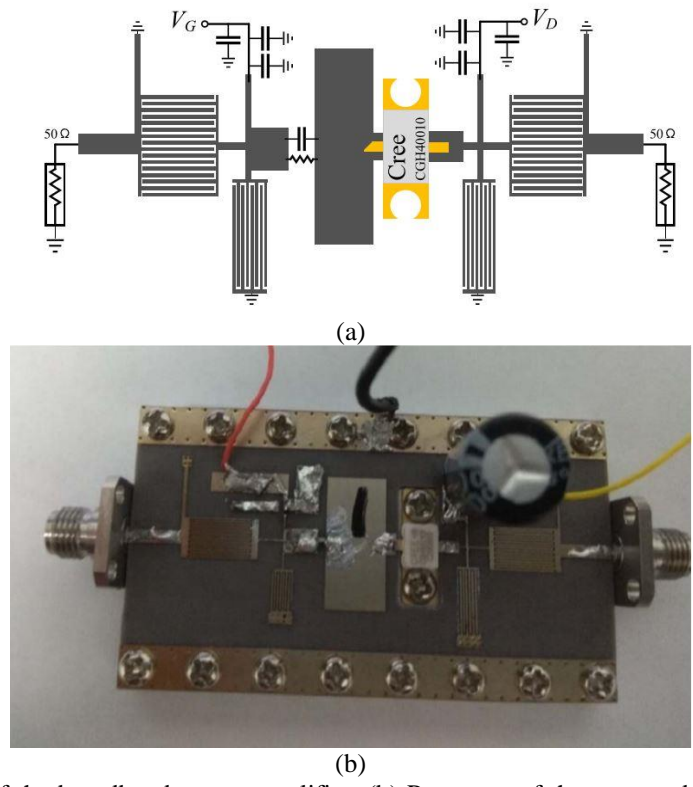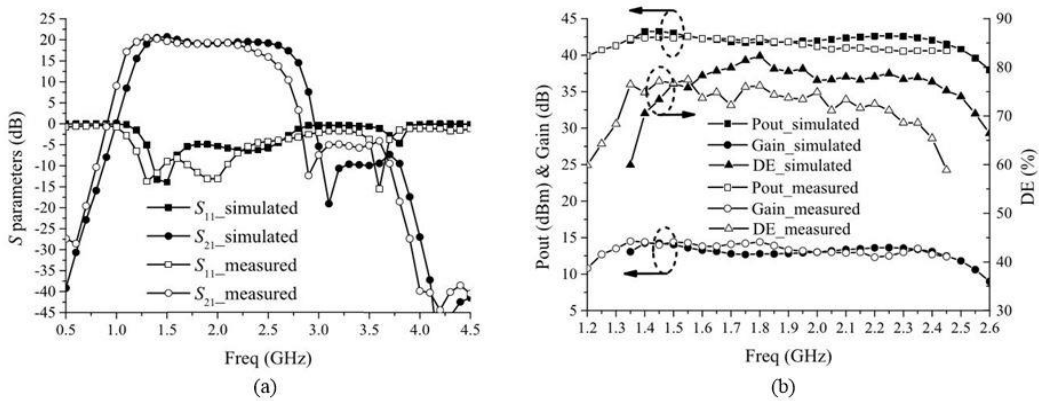

(a)

(b)

Figure 18. Performance of the broadband filter-amplifier in Figure 17. (a) Simulated and measured S_{11} and S_{21}; (b) Measured and simulated drain efficiency output power and gain versus frequency [42].

5. Comparison of integrated filter-amplifiers

A comparison of the state-of-the-art of the integrated filter-amplifiers is given in Table III. Various filter types (microstrip, DRs, waveguide, hybrid microstrip-to-DRs) together with their advantages/disadvantages are presented. The reviewed examples validate the generality of the filter-amplifier integration theory, which can be applied to both input or output complex impedances of active devices, as well as planar or non-planar filter constructions.

TABLE III
COMPARISON OF INTEGRATED FILTER-AMPLIFIERS IN OPEN LITERATURE

Filter Type	Cost	Loss	Volume	Ref.	Advantages & Disadvantages
Microstrip	Low	High	Medium	[4], [9] [33]-[37], [41]-[50]	Easy integration with on-chip transistor; Low cost; High loss
On-chip	High	High	Small	[37]	Extremely small volume; Easy integration with monolithic microwave integrated circuit; High loss; Costly
Dielectric resonator	Medium	Low	Large	[38]-[40]	Bulky; Complex planar-3D coupling structure; Low loss; Medium cost
Ceramic coaxial resonator	Medium	Low	Medium	[37]	High-Q factor; Low loss; Medium volume
SIW	Low	Medium	Medium	[21], [24]	Easy integration with on-chip transistor; Good trade-off between cost, loss and volume
EVA cylinder cavity	High	Low	Large	[23]	High cost; Bulky; Low loss at very high frequencies
Waveguide cavity	High	Low	Large	[19], [20]	Complex planar-3D coupling structure; High power capacity

6. Towards THz applications

The integrated filter-amplifier configuration can be particularly beneficial for THz applications where loss becomes a major concern. For THz amplifiers, the monolithic microwave integrated circuits (MMIC) are usually integrated with hollow metal waveguides. For such MMICs, the probe transitions are usually made from substrate materials such as alumina (dielectric constant of 9.6) or quartz (dielectric constant of 3.8). Due to the extremely sensitive parasitic parameters, there are stringent requirements on dimensional accuracy for these probes and waveguides. A common E-plane probe and a dipole antenna are illustrated in Figure 19 (a) and (b).

Instead of using separate matching networks, the active components can be matched directly using resonators of waveguide cavity filters, and such waveguide cavities have inherent low loss compared to typical matching circuitry based on lossy planar structures. This approach minimizes the footprint of the entire filter-amplifiers too. Although the concept of amplifiers matched to filters has been reported extensively, filter-amplifiers operating at THz frequencies have not been reported in the open literature yet. However, this method, i.e. using waveguide filters to match active/non-linear circuits with complex loads, has been successfully applied to the

design of millimetre-wave triplers [26]-[27] and terahertz sub-harmonic mixers [28]. During the co-designs of THz mixers and multipliers with waveguide cavity filters, the complex impedance of the diode chip is matched directly using waveguide filters. This new approach provides a built-in filtering function and removes the need for a separate impedance interface and therefore the associated transmission or transition losses. Excellent performance has been achieved for both the triplers and mixer, as shown in Figure 20 (a) and (b). Low-loss hollow waveguides are also widely used for the interconnection of multiple components in THz systems. Waveguide filters can be used to simultaneously match the output of one device and the input of the subsequent device, as shown in [51] and in Figure 20 (c) and (d), where the output of the 150 GHz frequency tripler and the input of the 300 GHz mixer are matched simultaneously by using the same 3rd-order waveguide filter. This offers a further reduction of the overall size of the system.
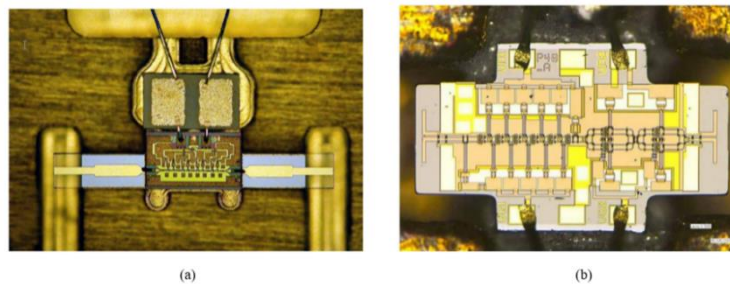

Figure 19. (a) A 300 GHz mHEMT amplifier using 2-mil-thick quartz E-plane probes [52]. (b) A 650 GHz power amplifier dipole antenna transition [53].

(a)

(b)

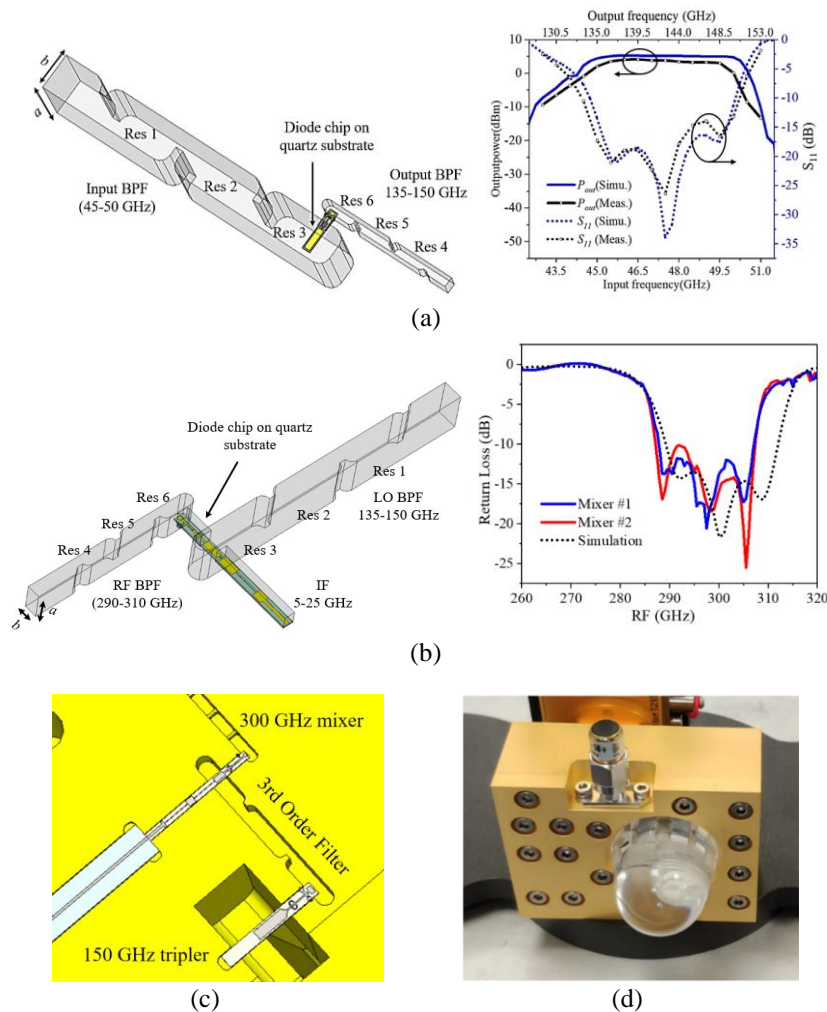(c)   (d)

Figure 20. (a) A 150 GHz tripler, matching directly using resonators of waveguide filters [26]; (b) A 300 GHz sub-harmonic mixer, matching directly using resonators of waveguide filters [28]; (c) An integrated sub-system based on the tripler in (a) and the mixer in (b); (d) A 300 GHz communication system front end in which the frequency triplers and mixers are based on structures shown in (a)-(c).

7. Conclusions

This article reviewed the concept of integrated filter-amplifiers and implementation examples. Various types of filters based on waveguide, SIW, microstrip and hybrid DR have been shown. This demonstrates the feasibility of replacing the conventional matching networks with filters. The integration techniques lead to more compact construction, lower loss and increased efficiency. As the transistors with complex port impedance/admittance can be matched with narrow/broadband filters, the methodology can be generalized to deal with a wide range of components with complex ports, such as antennas, mixers, and triplers. All these components can be eventually assembled to form a system and the technique is expected to be applicable to multi-functional devices and systems. There is still considerable work to be done in many aspects of this concept. The development of filter-amplifier integration techniques as well as other integrated devices and systems remains an active area of research.

References

[1]   D. M. Pozar, *Microwave Engineering*. Wiley, 2011.

[2]   I. J. Bahl, *Fundamentals of RF and Microwave Transistor Amplifiers*. Wiley, 2009.

[3]   J. S. Hong and M. J. Lancaster, *Microstrip Filters for RF/Microwave Applications*. Wiley, 2001.

[4]   X. Meng, C. Yu, Y. Liu, and Y. Wu, "Design approach for implementation of class-J broadband power amplifiers using synthesized band-pass and low-pass matching topology," *IEEE Trans. Microw. Theory Techn.,* vol. 65, no. 12, pp. 4984-4996, 2017, doi: 10.1109/TMTT.2017.2711021.

[5]   H. J. Carlin and J. J. Komiak, "A new method of broad-band equalization applied to microwave amplifiers," *IEEE Trans. Microw. Theory Techn.,* vol. 27, no. 2, pp. 93-99, 1979, doi: 10.1109/TMTT.1979.1129569.

[6]   B. S. Yarman and H. J. Carlin, "A simplified "Real frequency" technique appliable to broadband multistage microwave amplifiers," in *1982 IEEE MTT-S Int. Microwave Symp. Dig.*, 15-17 June 1982 1982, pp. 529-531, doi: 10.1109/MWSYM.1982.1130781.

[7]   R. M. Fano, "Theoretical limitations on the broadband matching of arbitrary impedances," *J. Franklin Inst.,* vol. 249, no. 2, pp. 139-154, 1950.

[8]   D. E. Dawson, "Closed-form solutions for the design of optimum matching networks," *IEEE Trans. Microw. Theory Techn.,* vol. 57, no. 1, pp. 121-129, 2009, doi: 10.1109/TMTT.2008.2009041.

[9]   P. Saad, C. Fager, H. Cao, H. Zirath, and K. Andersson, "Design of a highly efficient 2–4-GHz octave bandwidth GaN-HEMT power amplifier," *IEEE Trans. Microw. Theory Techn.,* vol. 58, no. 7, pp. 1677-1685, 2010, doi: 10.1109/TMTT.2010.2049770.

[10]   N. Tuffy, L. Guan, A. Zhu, and T. J. Brazil, "A simplified broadband design methodology for linearized high-efficiency continuous class-F power amplifiers," *IEEE Trans. Microw. Theory Techn.,* vol. 60, no. 6, pp. 1952-1963, 2012, doi: 10.1109/TMTT.2012.2187534.

[11]   J. Wang, S. He, F. You, W. Shi, J. Peng, and C. Li, "Codesign of high-efficiency power amplifier and ring-resonator filter based on a series of continuous modes and even–odd-mode analysis," *IEEE Trans. Microw. Theory Techn.,* vol. 66, no. 6, pp. 2867-2878, 2018, doi: 10.1109/TMTT.2018.2819650.

[12]   N. Kumar, C. Prakash, A. Grebennikov, and A. Mediano, "High-efficiency broadband parallel-circuit class E RF power amplifier with reactance-compensation technique," *IEEE Trans. Microw. Theory Techn.,* vol. 56, no. 3, pp. 604-612, 2008, doi: 10.1109/TMTT.2008.916906.

[13] J. Rooney, R. Parry, I. Hunter, and R. D. Pollard, "A filter synthesis technique applied to the design of multistage broad-band microwave amplifiers," *IEEE Trans. Microw. Theory Techn.,* vol. 50, no. 12, pp. 2947-2953, 2002, doi: 10.1109/TMTT.2002.805156.

[14] C. Chang and T. Itoh, "Microwave active filters based on coupled negative resistance method," *IEEE Trans. Microw. Theory Techn.,* vol. 38, no. 12, pp. 1879-1884, 1990, doi: 10.1109/22.64569.

[15] Y. Li *et al.*, "A novel low-power notch-enhanced active filter for ultrawideband interferer rejected LNA," *IEEE Trans. Microw. Theory Techn.,* vol. 69, no. 3, pp. 1684-1697, 2021, doi: 10.1109/TMTT.2021.3053264.

[16] Y. C. Li, K. C. Wu, and Q. Xue, "Power amplifier integrated with bandpass filter for long term evolution application," *IEEE Microw. Wirel. Compon. Lett.,* vol. 23, no. 8, pp. 424-426, 2013, doi: 10.1109/LMWC.2013.2268457.

[17] Y. S. Lin, J. F. Wu, W. F. Hsia, P. C. Wang, and Y. H. Chung, "Design of electronically switchable single-to-balanced bandpass low-noise amplifier," *IET Microw. Antennas Propag.,* vol. 7, no. 7, pp. 510-517, 2013, doi: 10.1049/iet-map.2012.0426.

[18] K. Wu and W. Meng, "A direct synthesis approach for microwave filters with a complex load and its application to direct diplexer design," *IEEE Trans. Microw. Theory Techn.,* vol. 55, no. 5, pp. 1010-1017, 2007, doi: 10.1109/TMTT.2007.895175.

[19] Y. Gao, J. Powell, X. Shang, and M. J. Lancaster, "Coupling matrix-based design of waveguide filter amplifiers," *IEEE Trans. Microw. Theory Techn.,* vol. 66, no. 12, pp. 5300-5309, 2018, doi: 10.1109/TMTT.2018.2871122.

[20] Y. Gao, X. Shang, C. Guo, J. Powell, Y. Wang, and M. J. Lancaster, "Integrated waveguide filter amplifier using the coupling matrix technique," *IEEE Microw. Wirel. Compon. Lett.,* vol. 29, no. 4, pp. 267-269, 2019, doi: 10.1109/LMWC.2019.2901892.

[21] Y. Gao *et al.*, "Substrate integrated waveguide filter–amplifier design using active coupling matrix technique," *IEEE Trans. Microw. Theory Techn.,* vol. 68, no. 5, pp. 1706-1716, 2020, doi: 10.1109/TMTT.2020.2972390.

[22] K. Chen, X. Liu, W. J. Chappell, and D. Peroulis, "Co-design of power amplifier and narrowband filter using high-Q evanescent-mode cavity resonator as the output matching network," in *2011 IEEE MTT-S Inter. Microw. Symp.*, 5-10 June 2011 2011, pp. 1-4, doi: 10.1109/MWSYM.2011.5972854.

[23] K. Chen, T. Lee, and D. Peroulis, "Co-design of multi-band high-efficiency power amplifier and three-pole high-Q tunable filter," *IEEE Microw. Wirel Compon. Lett.,* vol. 23, no. 12, pp. 647-649, 2013, doi: 10.1109/LMWC.2013.2283876.

[24] K. Chen, J. Lee, W. J. Chappell, and D. Peroulis, "Co-design of highly efficient power amplifier and high-Q output bandpass filter," *IEEE Trans. Microw. Theory Techn.,* vol. 61, no. 11, pp. 3940-3950, 2013, doi: 10.1109/TMTT.2013.2284485.

[25] Y. Gao, X. Shang, Y. Wang, and M. J. Lancaster, "An x-band waveguide orthomode transducer with integrated filters," *Microw. Opt. Technol. Lett.,* vol. 62, no. 1, pp. 78-81, 2020/01/01 2020, doi: 10.1002/mop.31986.

[26] C. Guo *et al.*, "A 135–150-GHz frequency tripler with waveguide filter matching," *IEEE Trans. Microw. Theory Techn.,* vol. 66, no. 10, pp. 4608-4616, 2018, doi: 10.1109/TMTT.2018.2855172.

[27] C. Guo *et al.*, "A 135–150-GHz frequency tripler using SU-8 micromachined WR-5 waveguides," *IEEE Trans. Microw. Theory Techn.,* vol. 68, no. 3, pp. 1035-1044, 2020, doi: 10.1109/TMTT.2019.2955684.

[28] C. Guo *et al.*, "A 290–310 GHz single sideband mixer with integrated waveguide filters," *IEEE Trans. THz Sci. Technol.,* vol. 8, no. 4, pp. 446-454, 2018, doi: 10.1109/TTHZ.2018.2841771.

[29] A. E. Atia and A. E. Williams, "Narrow-bandpass waveguide filters," *IEEE Trans. Microw. Theory Techn.,* vol. 20, no. 4, pp. 258-265, 1972, doi: 10.1109/TMTT.1972.1127732.

[30] R. J. Cameron, C. M. Kudsia, and R. R. Mansour, "Synthesis of Networks: Direct Coupling Matrix Synthesis Methods," in *Microwave Filters for Communication Systems: Fundamentals, Design, and Applications*: Wiley, 2018, pp. 247-294.

[31] R. R. Mansour, "High-Q tunable dielectric resonator filters," *IEEE Microw. Magaz.,* vol. 10, no. 6, pp. 84-98, 2009, doi: 10.1109/MMM.2009.933591.

[32] X. Shang *et al.*, "W-band waveguide filters fabricated by laser micromachining and 3-D printing," *IEEE Trans. Microw. Theory Techn.,* vol. 64, no. 8, pp. 2572-2580, 2016, doi: 10.1109/TMTT.2016.2574839.

[33] L. Gao, X. Y. Zhang, S. Chen, and Q. Xue, "Compact power amplifier with bandpass response and high efficiency," *IEEE Microw. Wirel. Compon. Lett.,* vol. 24, no. 10, pp. 707-709, 2014, doi: 10.1109/LMWC.2014.2340791.

[34] M. Furqan, F. You, W. Shi, S. Ahmad, and T. Qi, "A broadband power amplifier using hairpin bandpass filter matching network," *Electronics Lett.,* vol. 56, no. 4, 2019.

[35] M. F. Haider, F. You, T. Qi, and W. Shi, "A 10W broadband power amplifier with a hairpin resonator filter based on even-odd mode impedance analysis," in *2019 Europ. Microw. Conf. Central Europe (EuMCE)*, 13-15 May 2019, pp. 366-369.

[36] Z. Zhuang, Y. Wu, M. Kong, and W. Wang, "High-selectivity single-ended/balanced DC-block filtering impedance transformer and its application on power amplifier," *IEEE Trans. Circ. Systems I: Regular Papers,* vol. 67, no. 12, pp. 4360-4369, 2020, doi: 10.1109/TCSI.2020.3015883.

[37] J. A. Estrada, J. R. Montejo-Garai, P. d. Paco, D. Psychogiou, and Z. Popović, "Power amplifiers with frequency-selective matching networks," *IEEE Trans. Microw. Theory Techn.,* vol. 69, no. 1, pp. 697-708, 2021, doi: 10.1109/TMTT.2020.3020097.

[38] Q. Guo, X. Y. Zhang, J. Xu, Y. C. Li, and Q. Xue, "Bandpass class-F power amplifier based on multifunction hybrid cavity–microstrip filter," *IEEE Trans. Circ. Systerms II: Express Briefs,* vol. 64, no. 7, pp. 742-746, 2017, doi: 10.1109/TCSII.2016.2600575.

[39] J. Xu and X. Y. Zhang, "Dual-channel dielectric resonator filter and its application to doherty power amplifier for 5G massive MIMO system," *IEEE Trans. Microw. Theory Techn.,* vol. 66, no. 7, pp. 3297-3305, 2018, doi: 10.1109/TMTT.2018.2829197.

[40] J. Xu, X. Y. Zhang, and X. Song, "High-efficiency filter-integrated class-F power amplifier based on dielectric resonator," *IEEE Microw. Wirel. Compon. Lett.,* vol. 27, no. 9, pp. 827-829, 2017, doi: 10.1109/LMWC.2017.2734778.

[41] P. Wright, J. Lees, J. Benedikt, P. J. Tasker, and S. C. Cripps, "A methodology for realizing high efficiency class-J in a linear and broadband PA," *IEEE Trans. Microw. Theory Techn.,* vol. 57, no. 12, pp. 3196-3204, 2009, doi: 10.1109/TMTT.2009.2033295.

[42] Q. Cai, W. Che, G. Shen, and Q. Xue, "Wideband high-efficiency power amplifier using D/CRLH bandpass filtering matching topology," *IEEE Trans. Microw. Theory Techn.,* vol. 67, no. 6, pp. 2393-2405, 2019, doi: 10.1109/TMTT.2019.2909892.

[43] G. Nikandish, R. B. Staszewski, and A. Zhu, "Broadband fully integrated GaN power amplifier with embedded minimum inductor bandpass filter and AM–PM compensation," *IEEE Solid-State Circ. Lett.,* vol. 2, no. 9, pp. 159-162, 2019, doi: 10.1109/LSSC.2019.2927855.

[44] Z. Su, C. Yu, B. Tang, and Y. Liu, "Bandpass filtering power amplifier with extended band and high efficiency," *IEEE Microw. Wirel. Compon. Lett.,* vol. 30, no. 2, pp. 181-184, 2020, doi: 10.1109/LMWC.2020.2966067.

[45] M. Yang, J. Xia, Y. Guo, and A. Zhu, "Highly efficient broadband continuous inverse class-F power amplifier design using modified elliptic low-pass filtering matching network," *IEEE Trans. Microw. Theory Techn.,* vol. 64, no. 5, pp. 1515-1525, 2016, doi: 10.1109/TMTT.2016.2544318.

[46] A. Grebennikov, "High-efficiency class-E power amplifier with shunt capacitance and shunt filter," *IEEE Trans. Circ. Systems I: Regular Papers,* vol. 63, no. 1, pp. 12-22, 2016, doi: 10.1109/TCSI.2015.2512698.

[47] K. Chen and D. Peroulis, "Design of highly efficient broadband class-E power amplifier using synthesized low-pass matching networks," *IEEE Trans. Microw. Theory Techn.,* vol. 59, no. 12, pp. 3162-3173, 2011, doi: 10.1109/TMTT.2011.2169080.

[48] Z. Zhuang, Y. Wu, Q. Yang, M. Kong, and W. Wang, "Broadband power amplifier based on a generalized step-impedance quasi-Chebyshev lowpass matching approach," *IEEE Trans. Plas. Sci.,* vol. 48, no. 1, pp. 311-318, 2020, doi: 10.1109/TPS.2019.2954494.

[49]   S. Zarghami, M. Hayati, M. K. Kazimierczuk, and H. Sekiya, "Continuous class-F power amplifier using quasi-elliptic low-pass filtering matching network," *IEEE Trans. Circ. Systems II: Express Briefs,* vol. 67, no. 11, pp. 2407-2411, 2020, doi: 10.1109/TCSII.2020.2964895.

[50]   H. Kang *et al.*, "Optimized broadband load network for doherty power amplifier based on bandwidth balancing," *IEEE Microw. Wirel. Compon. Lett.,* vol. 31, no. 3, pp. 280-283, 2021, doi: 10.1109/LMWC.2020.3043770.

[51]   M. J. Lancaster *et al.*, "GaAs schottky components for 300 GHz communication systems using a resonator impedance matching approach," in *2019 44th Inter. Conf. Infrared, Millim. THz Waves (IRMMW-THz)*, 1-6 Sept. 2019 2019, pp. 1-1, doi: 10.1109/IRMMW-THz.2019.8874014.

[52]   A. Tessmann *et al.*, "A 300 GHz mHEMT amplifier module," in *2009 IEEE Inter. Conf. InP Related Mater.*, 10-14 May 2009 2009, pp. 196-199, doi: 10.1109/ICIPRM.2009.5012477.

[53]   V. Radisic, K. M. K. H. Leong, X. Mei, S. Sarkozy, W. Yoshida, and W. R. Deal, "Power amplification at 0.65 THz using InP HEMTs," *IEEE Trans. Microw. Theory Techn.,* vol. 60, no. 3, pp. 724-729, 2012, doi: 10.1109/TMTT.2011.2176503.